Cellular Microbiology (2016) **18**(1), 125–136
doi:10.1111/cmi.12491
First published online 31 August 2015

Modulation of cell surface transport and lipid raft localization by the cytoplasmic tail of the influenza virus hemagglutinin

Silvia Scolari,[1] Katharina Imkeller,[1] Fabian Jolmes,[1] Michael Veit,[2] Andreas Herrmann[1] and Roland Schwarzer[1,3]*

[1]*Department of Biology, Molecular Biophysics, Humboldt University Berlin, 10115 Berlin, Germany.*
[2]*Department of Immunology and Molecular Biology, Free University, 14163 Berlin, Germany.*
[3]*Department of Biological Chemistry, Weizmann Institute of Science, 76100 Rehovot, Israel.*

Summary

Viral glycoproteins are highly variable in their primary structure, but on the other hand feature a high functional conservation to fulfil their versatile tasks during the pathogenic life cycle. Typically, all protein domains are optimized in that indispensable functions can be assigned to small conserved motifs or even individual amino acids. The cytoplasmic tail of many viral spike proteins, although of particular relevance for the virus biology, is often only insufficiently characterized. Hemagglutinin (HA), the receptor-binding protein of the influenza virus comprises a short cytoplasmic tail of 13 amino acids that exhibits three highly conserved palmitoylation sites. However, the particular importance of these modifications and the tail in general for intracellular trafficking and lateral membrane organization remains elusive. In this study, we generated HA core proteins consisting of transmembrane domain, cytoplasmic tail and a minor part of the ectodomain, tagged with a yellow fluorescent protein. Different mutation and truncation variants of these chimeric proteins were investigated using confocal microscopy, to characterize the role of cytoplasmic tail and palmitoylation for the intracellular trafficking to plasma membrane and Golgi apparatus. In addition, we assessed raft partitioning of the variants by Foerster resonance energy transfer with an established raft marker.

We revealed a substantial influence of the cytoplasmic tail length on the intracellular distribution and surface exposure of the proteins. A complete removal of the tail hampers a physiological trafficking of the protein, whereas a partial truncation can be compensated by cytoplasmic palmitoylations. Plasma membrane raft partitioning on the other hand was found to imperatively require palmitoylations, and the cysteine at position 551 turned out to be of most relevance.

Our data shed further light on the tight interconnection between cytoplasmic elements and intracellular trafficking and suggest a function of HA palmitoylations in both lateral sorting and anterograde trafficking of the glycoprotein.

Received 27 March, 2015; revised 28 June, 2015; accepted 13 July, 2015. *For correspondence. E-mail Roland-Schwarzer@gmx.de; Tel. (+49) 30 2093 8860; Fax (+49) 30 2093 8585.

Introduction

Enveloped viruses are highly diverse and significantly differ in many aspects of their life cycle, and also in their molecular structure and organization. However, the infection process of all members of this group of pathogens entails fusion of the viral membrane with the host membrane, leading to the release of virus genome into the cytosol. The necessity to mediate membrane fusion during virus entry gives rise to a high functional homology of the respective surface proteins. Therefore, viral membrane-fusion glycoproteins share some general structural features. Typically, they are composed of an ectodomain, which is often involved in the binding of the cellular receptor, anchored into the lipid bilayer through a transmembrane domain (TMD) that terminates with a cytoplasmic tail (CT) with miscellaneous functions. Viral fusion proteins are mainly divided into two classes: the first comprehending glycoproteins of orthomyxoviruses, paramyxoviruses, retroviruses, filoviruses and coronaviruses; the second including those of flaviviruses and togaviruses (Kielian and Rey, 2006). The glycoprotein B of herpes simplex virus and the glycoprotein G of vesicular stomatitis virus form a third separate class (Backovic and Jardetzky, 2011). Class I ectodomain glycoproteins form trimers with a triple coiled-coil stem, which, in the post-fusion state, gives a distinctive six-helix bundle. Their active fusogenic form is obtained through a proteolytic cleavage that reveals the

hydrophobic fusion peptide (Steven and Spear, 2006). The ectodomain of influenza virus hemagglutinin (HA) was the first fusion mediating virus spike protein being structurally resolved (Wilson *et al.*, 1981).

In the last decades, the main characteristics of the extracellular domains of different viral proteins have been extensively described, whereas often the role of the transmembrane and cytoplasmic domains remained elusive. Recently, more and more studies have been focused on the intracellular and transmembrane portion of such proteins, to provide a better understanding of their biological significance and function. Nowadays, it is clear that these domains act not only as an anchor for the ectodomain. Indeed, with respect to influenza virus, several groups demonstrated on one side that the length of the TMD is critical for fusion pore formation (Armstrong *et al.*, 2000), and on the other side that CT and TMD are involved in lipid raft targeting of HA (Scheiffele *et al.*, 1997; Scolari *et al.*, 2009; Engel *et al.*, 2010). The CT, was furthermore shown to be involved in viral particle formation (Jin *et al.*, 1997; Zhang *et al.*, 2000), and also to be dispensable for HA transport and stability (Doyle *et al.*, 1986). It was proposed that the HA and neuraminidase CTs may interact with other viral components and may permit the recruitment of the matrix protein M1 to the viral envelope (Ali *et al.*, 2000). Investigation on other viruses also reported a role of the glycoprotein CTs in fusion and viral entry (Januszeski *et al.*, 1997; Harman *et al.*, 2002) as well as in the production of an infective progeny (Brack *et al.*, 2000; Murakami and Freed, 2000; Oomens *et al.*, 2006).

Of peculiar relevance are the three cytoplasmic cysteins of HA that were demonstrated to be S-acylated by one stearic acid residue and two palmitic acid residues (Kordyukova *et al.*, 2008). Lipid attachment is a common post-translational modification within integral and peripheral membrane proteins, and fatty-acylated proteins are involved in many cellular processes such as vesicular trafficking and fusion (Veit *et al.*, 1996), signalling (Smotrys and Linder, 2004) and protein sorting (Greaves and Chamberlain, 2007). In addition, S-acylation also functions as a membrane anchor; e.g. it promotes the attachment of the SNARE SNAP-25 to the cell plasma membrane (PM) (Veit *et al.*, 1996; Greaves and Chamberlain, 2007). Many viral proteins become fatty acylated after synthesis, and the function of such modification has still to be fully understood. Taken together, these premises led to the idea that viral CTs and their peculiar characteristics, such as fatty acylation, may represent a key regulatory mechanism of viral protein trafficking and lateral membrane organization. Here, we employed the transmembrane and cytoplasmic domain of HA as a target for genetic manipulation, to unravel the relevance of the CT and S-acylation in HA intracellular trafficking and lateral membrane sorting.

Results

Trafficking of fluorescent hemagglutinin chimeric proteins

The main purpose of this study was the investigation of the role of the HA CT and TMD for intracellular trafficking and lateral membrane arrangement in living cells. To this end, we used fluorescently tagged chimera of HA of A/FPV/Rostock/34 (H7N1) for which the ectodomain was essentially replaced by a fluorescent protein. We have recently introduced this type of chimera to study HA raft partitioning in a live-cell system (Scolari *et al.*, 2009). The advantage of those constructs is that any interference of the rather large mYFP with the function of the small cytoplasmic domain is avoided. Furthermore, the lack of the full HA ectodomain allows to judge exclusively the importance of the CT for trafficking and lateral membrane arrangement that might become masked by (dominating) properties of the ectodomain. Nevertheless, when considering intracellular transport and membrane organization of the full-length HA, the ectodomain has to be born in mind as well (Discussion section).

HAmYFP enters the exocytic pathway. First, we conducted an extensive characterization of the protein HAmYFP by fluorescence microscopy. This construct is a derivative of the native HA comprising wild type sequences of the entire CT, TMD and the membrane-proximal region of the ectodomain and will be termed wt in the following. As demonstrated by confocal microscopy (Fig. 1), wt shows the typical fluorescence pattern of a protein in transit along the exocytic pathway. A minor spatial correlation was found upon endoplasmic reticulum co-staining using ER-Tracker Red (Invitrogen, Carlsbad, CA) (Fig. 1A), indicative of a physiological folding and thus efficient ER exit of the chimeric protein. Co-localization on the other hand was found with Golgi-turquoise and GPImCFP, serving as marker of the Golgi apparatus and the plasma membrane respectively (Fig. 1B and C). No co-localization was found with the endocytosis marker Rab5-turquiose (Fig. 1D) suggesting that wt is not, or only to a small extent, re-internalized by endocytosis. This localization is in agreement with previous studies on full-length HA (Rindler *et al.*, 1984; Rodriguez-Boulan *et al.*, 1984; Doyle *et al.*, 1985; Copeland, 1986; Gottlieb *et al.*, 1986; Veit *et al.*, 1991; Garten *et al.*, 1992). Nevertheless, for comparison, we also expressed unlabeled, full-length HA for subsequent immunofluorescence analysis and found a comparable intracellular distribution of the generic wild type and our chimeric variant. As HAmYFP, the unlabeled HA localized predominantly to plasma membrane and Golgi apparatus (Figure S1 and Figure S2) and showed a high ratio of plasma membrane exposure to overall expression (Figure S1). Therefore, we conclude that our wild type represents a relevant model of its physiological counterpart in the context of protein trafficking.

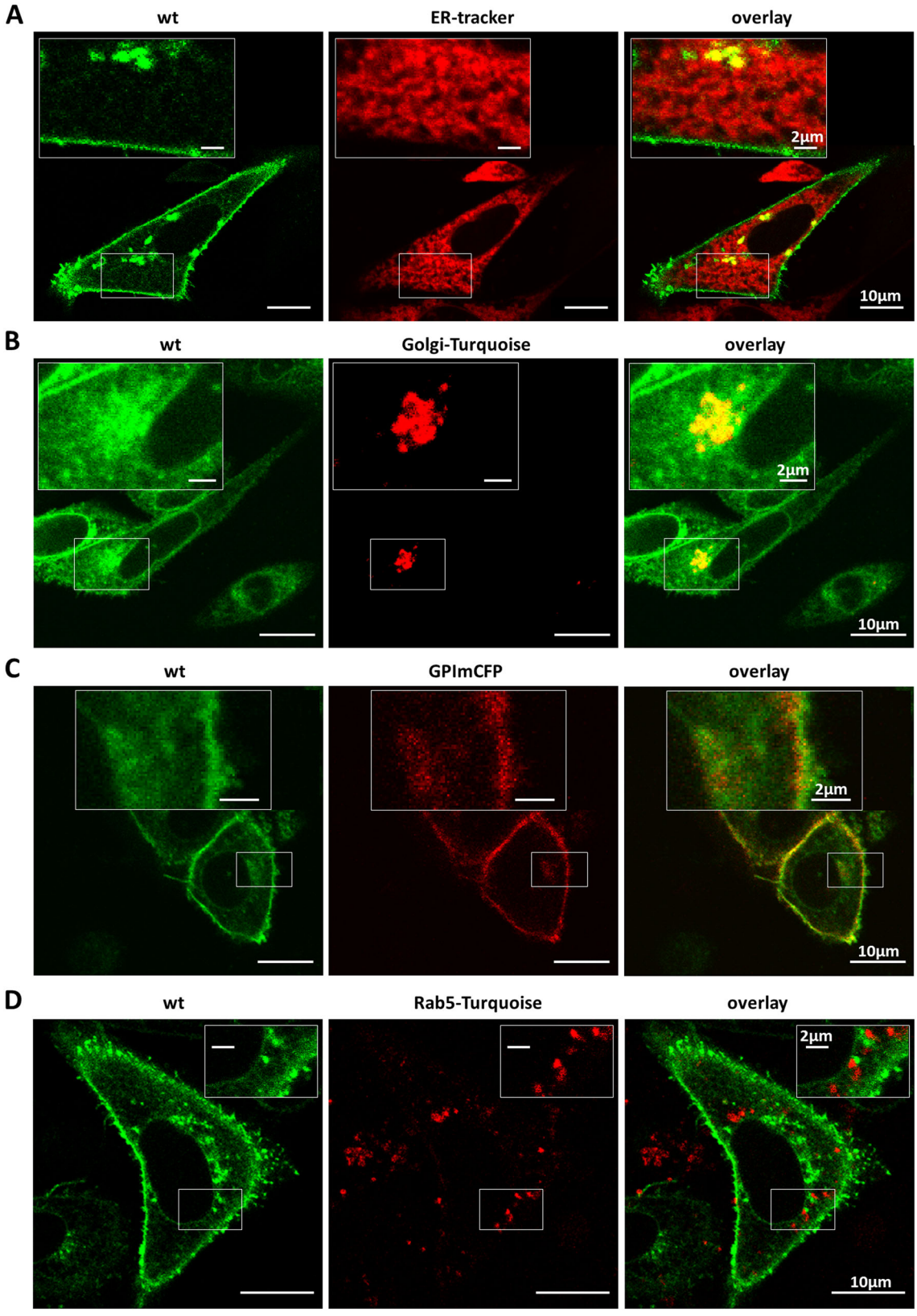

Fig. 1. Microscopic characterization of HAmYFP. Confocal images of CHO-K1 cells transfected with HAmYFP (wt), (A) upon staining with ER-Tracker Red or upon co-transfection with the proteins (B) Golgi-turquoise, (C) GPImCFP or (D) Rab5-turquoise, serving as a marker of the Golgi apparatus, the plasma membrane and endocytic vesicles respectively. Insets show a magnified region of the boxed area.

Cytoplasmic tail truncation variants of the chimeric hemagglutinin are excluded from the plasma membrane. To pinpoint specific motifs and protein domains that are involved in HA trafficking and subcellular localization, different truncation and mutation variants of wt were generated. At first, a construct was generated that contained only the TMD but lacked the whole CT and even the membrane-proximal region of the ectodomain (Fig. 2A, TMD). Secondly, the TMD was progressively shortened of one, two or three residues at its C-terminus (Fig. 2, TMD-1, TMD-2 and TMD-3). CHO-K1 cells were transfected with the chimera, and the intracellular distribution was investigated by confocal microscopy upon co-expression of the plasma membrane marker GPImCFP. However, all four mutants were found to be excluded from the cell surface (Fig. 3B–D), an observation that was confirmed by quantitative images analysis (Fig. 4) and by comparison with cells co-expressing GPImCFP and the chimeric protein HAmYFP (Fig. 1). This result was rather unexpected because in a previous study by Doyle (Doyle *et al*., 1986), full-length HA mutants lacking the whole CT and even portions of the TMD were still efficiently transported to the cell surface. The main difference between our constructs and the one presented by Doyle is the absence of the ectodomain including the seven glycosylation sites and the putative raft targeting motif VIL (Takeda *et al*., 2003; Engel *et al*., 2012). Based on the fact that HA glycosylation is supposed to be important for folding, trimerization, stability and efficient transport of the protein (Roberts *et al*., 1993; Wagner *et al*., 2002), several residues including the glycosylation site N496 were added to the N-terminus of the TMD (scheme in Fig. 2). This new mutant, named TMD + ED, containing one glycosylation site (N496) but still lacking the CT was then co-transfected with the plasma membrane marker GPImCFP in CHO cells. As the other CT truncation variants, the construct was found to be exclusively localized in the ER (Figs 3E and 4), demonstrating that the CT is stringently required for cell surface transport of the HA chimeras and that neither N496 nor VIL are able to rescue their intracellular trafficking defect in absence of the CT.

Palmitoylation and cytoplasmic tail length affect transport to the plasma membrane. To further investigate the role of cytoplasmic residues in the intracellular trafficking of HA chimeras, we successively reintroduced different fractions of the CT. The focus of this approach is on the cytoplasmic cysteines because the palmitoylations of those residues, as reported for different other proteins (Greaves and Chamberlain, 2007; Hundt *et al*., 2009; Veit, 2012), are surmised to interfere with intracellular trafficking and other protein activities. Our CT truncation variants comprised either one or two palmitoylation sites respectively, whereas the wild type contained all three. The constructs Δ1, which was lacking the C-terminal palmitoylation site, but included C551 and C559, and Δ2, which was lacking two acylation sites, thus including only residue C551 (scheme in Fig. 2B, Δ1 and Δ2) were co-transfected with

Fig. 2. HA constructs used in this study. The TMD-HA chimeric protein wt was modified by site-directed mutagenesis and truncation to generate different variants (A–C). From left to right are highlighted in the scheme: the link to YFP (···) in grey, the beginning of the HA amino acids (492), the ectodomain (italic), glycosylation site N496 (underlined), the cytoplasmic tail (bold), palmitoylation sites (red) and a conserved arginine (blue). The numeration corresponds to influenza A virus (strain A/Fowl plague virus/Rostock/8/1934 H7N1), uniprot entry: P03459.

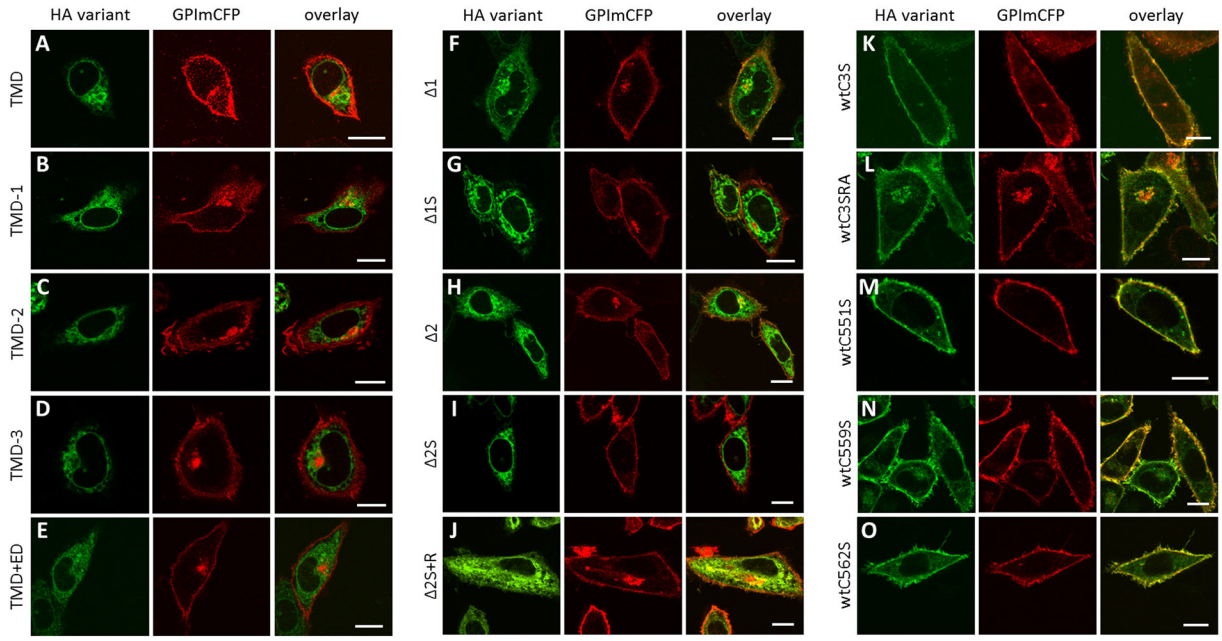

Fig. 3. Confocal images of CHO-K1 cells co-transfected with HA variants and the plasma membrane marker GPImCFP. The figure displays equatorial slices of representative cells expressing TMD variants of HA (left panel (A–E)), cytoplasmic tail truncation variants and their respective palmitoylation mutants (middle panel (F–J)), and different palmitoylation mutants still comprising an otherwise unchanged cytoplasmic tail (right panel (K–O)). For all proteins, co-localization between the respective HA variant and GPImCFP appears orange in the overlay images. Scale bars = 10 μm.

GPImCFP in CHO cells. Both proteins were found to be efficiently transported to the plasma membrane, but in contrast to wt, also highly localized intracellularly (Figs 3F and H and 4). To prove that this difference in the localization between the CT truncation variants and wt is reflective of an exocytosis defect rather than of an increased re-internalization of the protein, we performed another set of co-staining assays (Fig. S3). Co-localization of the Δ2 variant was found with markers for ER and Golgi apparatus but not the endocytosis-related protein Rab5. This finding indicates that the reintroduction of some CT residues partly restored the correct delivery of the proteins to the plasma membrane, thus pointing to a relevant role of the HA CT for stability and efficient exocytic transport.

It was further interesting to elucidate whether palmitoylation has an influence on the cellular localization of the protein because it has recently been reported that an impaired S-acylation leads to an accumulation of proteins in the Golgi apparatus (Hundt *et al.*, 2009). We therefore produced mutants of Δ1 and Δ2 named Δ1S and Δ2S (Fig. 2B). In both cases, the cysteine at position 551 was mutated to serine. Whereas mutant Δ1S was still almost as efficiently transported to the cell surface as Δ1 (Figs 3G and 4), the protein Δ2S was almost exclusively retained into the ER and only slightly visible in Golgi apparatus and at the PM (Figs 3I and 4). This result was rather surprising given the fact that the protein wtC3S, a mutant in which the three acylation sites were mutated to serines (Fig. 1C), but still

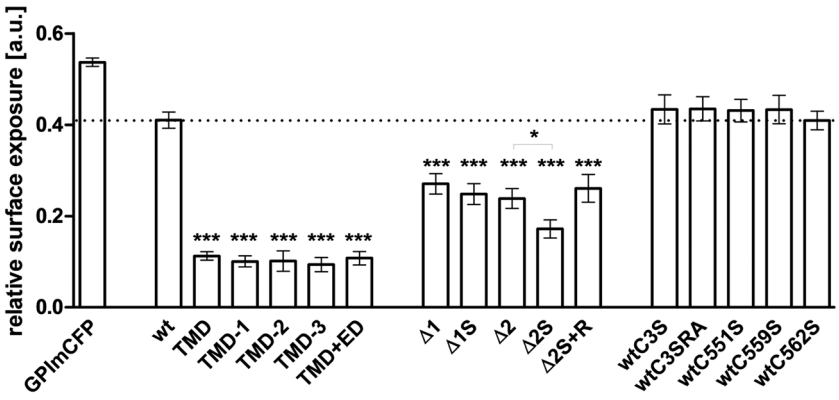

Fig. 4. The relative surface exposure of the different HA variants assessed by image analysis. Regions of interest were initially defined in GPImCFP images of CHO-K1 cells co-expressing HA variants to select for plasma membrane and the whole cell. The relative surface exposure was then calculated as ratio between plasma membrane staining and overall expression by analysing background corrected confocal images. Each bar represents the average of 10–20 cells with standard error of the mean (SEM). If not otherwise stated, statistical significance compared with wt is displayed $^{***}P < 0.001$ and $^{*}P = 0.01$–0.05.

conserving the CT full-length, was clearly transported to the cell surface (Figs 3K and 4). From a sequence alignment of C3S, Δ1, Δ2, Δ1S and Δ2S sequences (Fig. 2), R558 was identified as putative residue responsible for ensuring cell surface transport of the protein. To verify such hypothesis, we added R558 to Δ2S, and we mutated it in the C3S sequence thus producing Δ2S + R and wtC3SRA proteins (Fig. 2B and C). The point mutation did not have any effect on C3S transport (Figs 3 and 4); however, cell surface delivery was recovered in Δ2S + R (Figs 3J and 4). These results indicate that both the length of the CT and the presence of palmitoylated residues are crucial features ensuring stability and surface transport of HA.

Lateral organization of hemagglutinin chimeric proteins

In order to elucidate the role of the CT and palmitoylation in raft association of HA, we conducted fluorescence lifetime imaging microscopy (FLIM) experiments in living cells as described previously (Zacharias *et al*., 2002; Scolari *et al*., 2009; Schwarzer *et al*., 2014). Briefly, FLIM was used to report Foerster resonance energy transfer (FRET) between GPImCFP, serving as a raft marker, and the YFP-tagged HA chimeras. As it is highly distance dependent, occurring FRET was shown to report a co-clustering of both fluorescently labelled protein species in nanodomains, an approach that has been previously applied by us, to rationalize raft partitioning of different viral proteins including HAmYFP (Scolari *et al*., 2009; Schwarzer *et al*., 2014). For this construct, we also demonstrated that raft partitioning is abrogated upon depletion of cholesterol, a crucial component of plasma membrane lipid rafts (Scolari *et al*., 2009).

C551 is the key palmitoylation site for the plasma membrane lipid raft partitioning of hemagglutinin chimera. For both proteins, Δ1 and Δ2, FRET efficiencies were found to be in the order of the wild type protein HAmYFP (Fig. 5) indicating no effect of the CT truncation on the raft partitioning of chimeric HA. To investigate more specifically the function of C551, the proteins Δ1S and Δ2S + R, being deficient in this particular residue, were subjected to FLIM-FRET analysis. Upon co-expression with the raft marker, energy transfer was for both proteins in the background level thus indicating an essential role of C551 in raft clustering of HA (Fig. 5). Subsequently, to verify the validity of our raft partitioning results, we performed a clustering analysis of our FLIM-FRET data. This approach allows distinguishing false-positive FRET by plotting the FRET efficiency of individual cells against their respective acceptor intensity. If energy transfer is a result of random interactions between the raft marker GPImCFP and the YFP-tagged protein under study, a linear relationship should be obtained, and high FRET efficiencies should be

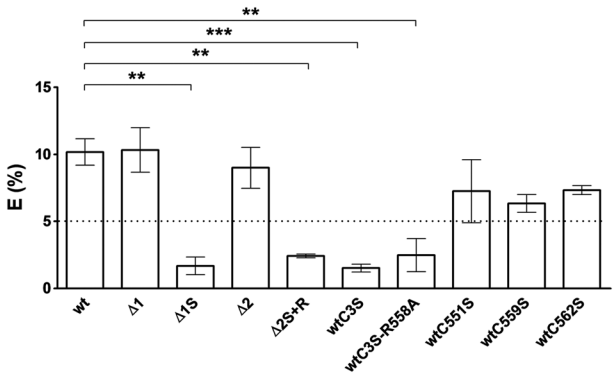

Fig. 5. Plasma membrane raft partitioning analysis by FLIM-FRET. Plasma membrane FRET efficiencies calculated from lifetime measurements of at least three independent experiments with at least 30 cells analysed for each protein under study. All bar charts display FRET efficiencies in percent with SEM. Statistical significance is shown by (***) $P < 0.001$ and (**) $P = 0.001$–0.01. For visualization, a dashed line is drawn to distinguish raft partitioning and raft excluded protein variants (SEM above and below the line).

only achieved at high acceptor intensities (Zacharias *et al*., 2002; Scolari *et al*., 2009; Schwarzer *et al*., 2014). This raft-clustering analysis was conducted with four variants possessing a moderate and high plasma membrane expression; wt, Δ1, Δ2 and Δ2S + R (compare Figs 3 and 4). As expected, only the latter displayed a linear relationship, whereas the three other variants showed a raft-clustering dependent FRET (Fig. S4). This finding was further supported by fitting the data to a simple saturable binding model (Fig. S4) as described by Zacharias *et al*. To further pinpoint the molecular background of the HA raft partitioning, we produced the mutants wtC551S, wtC559S and wtC562S (scheme in Fig. 2C). Upon co-transfection with GPImCFP, we could observe a slight, although not significant reduction of the energy transfer for all cysteine mutants (Fig. 5) in the respective FLIM-FRET experiments. The variants wtC3S and wtC3SRA on the other hand were found to cause significantly lower FRET than the wild type HAmYFP (Fig. 5). This observation suggests that, in general, the palmitoylations of the residues C551, C559 and C562 ensure plasma membrane raft clustering. However, whereas the fatty acid attached to C551 alone is sufficient to permit raft partitioning (Fig. 5, Δ2), a loss of this residue can be compensated by both (Fig. 5, wtC551S) but not by a single (Fig. 5, Δ1S) palmitoylated cysteine.

Although it has been shown before that overexpressed HA is efficiently and completely acylated even upon introduction of mutations and truncations (Brett *et al*., 2014), we performed radioactive palmitic acid labelling, revealing that Δ1 is indeed palmitoylated as well as the mutant wtC559S and wt, taken as examples, whereas

no palmitic acid band is visible for wtC3S mutant (Figure S5; Scolari *et al*., 2009). Furthermore, we analysed the donor–acceptor ratio of our chimeric proteins and found that within different experiments, the relative level of expression of GPImCFP to the respective HA variant did not significantly vary (Fig. S6) indicating that differences in the protein expression level do not account for the obtained differences in the raft partitioning of the various HA chimeric constructs.

Hemagglutinin is partitioning in lipid raft in the Golgi apparatus. In recent years, the hypothesis was raised that lipid rafts and consequently also a nanodomain-dependent lateral protein sorting already emerge in internal membranes such as the Golgi apparatus (Campbell *et al*., 2002; Resh, 2004; Vetrivel *et al*., 2004; Simons and Sampaio, 2011; Surma *et al*., 2012). To address this question, we analysed lateral clustering of our four major HA variants; wt, Δ1, Δ2 and C3S with the raft marker GPImCFP in the Golgi apparatus utilizing the FLIM-FRET approach described before (Fig. 6). In agreement with the Golgi-raft hypothesis, we found raft partitioning for wt, whereas the C3S variant could be again demonstrated to be excluded. Interestingly, in contrast to our findings from plasma membrane FLIM-FRET, the variants Δ1 and Δ2 displayed a decrease in the raft partitioning as a result of the conducted truncations. Although there is no statistically significant difference between the wt and Δ1 or Δ1 and Δ2, the successive drop of the FRET efficiencies might indicate a partial attenuation of the Golgi apparatus raft association by the removal of parts of the CT.

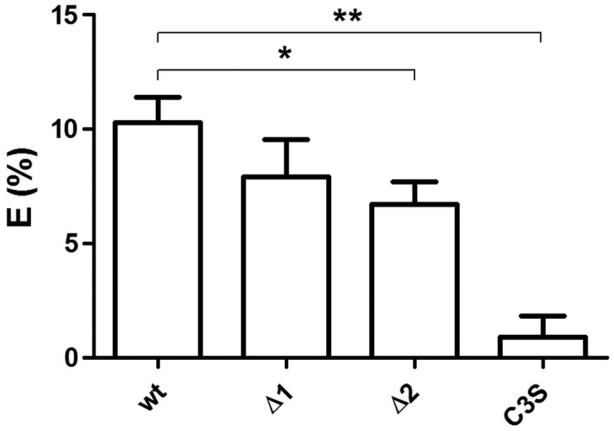

Fig. 6. Raft partitioning in the Golgi apparatus. Plasma membrane FRET efficiencies calculated from lifetime measurements of at least two independent experiments with at least 15 cells analysed for each protein under study. All bar charts display average FRET efficiencies in percent with SEM. Statistical significance is shown by (**) $P = 0.001–0.01$ and (*) $P < 0.05$.

Discussion

This work aimed at shedding further light on the function of the CT of viral spike proteins at the example of the influenza glycoprotein HA. HA is of particular interest because of its very short and highly conserved CT. Indeed, it can be surmised that it possesses a high functional density. If so, the experimental advantage is that only a few changes have to be introduced by genetic manipulation of the amino acid sequence to thoroughly investigate the CT's role in specific protein properties. Based on this consideration, we scrutinized the role of the CT length in the intracellular trafficking as well as its relevance for PM delivery of the protein. We further characterized the impact of the three cytoplasmic palmitoylations on the surface exposure as well as raft association of the protein. For an overview, constructs and results are summarized in Table 1. Of note, our wt construct (HAmYFP) was demonstrated to resemble its native counterpart in terms of intracellular localization and surface exposure. This observation indicates that this construct represents a suitable model for the full-length HA and thus enables investigation of CT and TMD properties without interference by elements in the HA ectodomain.

First, we observed that removing the entire CT had a dramatic effect on intracellular trafficking, leading to the arrest of the proteins at an early stage of transport or processing, hence compromising the movement to the Golgi apparatus (TMD constructs: Figs 2A, 3A–D and 4). A reintroduction of 34 residues belonging to the ectodomain did not restore the delivery of the protein to the cell surface (TMD + ED: Figs 2A, 3E and 4). We conclude that in the absence of the CT, neither N496 nor VIL are able to rescue trafficking of our chimeric proteins. This observation does not necessarily also apply to full-length HA because in the context of an intact HA ectodomain, both N496 and VIL might have a more pronounced impact on protein folding and trafficking. Nevertheless, we observed, although to a lower extent than the wt, efficient transport of the protein to the PM when seven residues of the CT were reinserted (Δ2: Figs 2B, 3H and 4). Among these, the palmitoylation site C551 was of particular importance. Indeed, we observed that abolition of the palmitoylation by exchange of cysteine with serine again impaired the correct transport of the construct (Δ2S: Figs 3I and H and 4). On the other hand, palmitoylation mutants, i.e. wtC551S, wtC559S, wtC562S and in particular the triple mutants wtC3S and wtC3SRA with an otherwise conserved CT, did not show any particular transport impairment (Scolari *et al*., 2009; Figs 3K, 3K–O and 4). Taken together, these findings clearly indicate that the CT palmitoylations are of subsidiary relevance for the plasma membrane targeting

Table 1. Summary of used constructs and obtained results.

	wt	TMD	TMD-1	TMD-2	TMD-3	TMD+ED	Δ1	Δ1S	Δ2	Δ2S	Δ2S+R	wtC3S	wtC3SRA	wtC551S	wtC559S	wtC562S
C551S	■						■		■						■	■
C559S	■						■	■						■		■
C562S	■													■	■	
Surface exposure	+++	-	-	-	-	-	++	++	++	-	++	+++	+++	+++	+++	+++
Raft partitioning	+	n.a.	n.a.	n.a.	n.a.	n.a.	+++	-	+++	n.a.	-	-	-	+++	+++	+++

The fluorescently labelled variants used in this study are arranged in columns with their respective properties assigned in rows. In the first three rows, grey filling denotes presence of the respective palmitoylation site, stated on the left. The next row displays the surface exposure of the constructs as described in the text and displayed in Fig. 4. +++, ++ and – were assigned according to relative surface exposure of $>$ 0.4, 0.2–0.4 and below 0.2. The last row summarizes the results of the plasma membrane raft partitioning experiments with + being reflective of a raft association, - representing non-raft proteins and n.a. indicating proteins that could not be studied for this properties because of failure of transport to the plasma membrane.

of the protein. Nevertheless, they appear to rescue trafficking defects of CT truncations, and therefore, we surmise that there must be a sort of synergism between the length and palmitoylation of the CT. The palmitoylation may somehow compensate deletions of the CT that otherwise would hamper an efficient, intracellular transport. For example, the presence of the whole CT fragment may help the correct folding and stretching of the TMD, in order to span the lipid bilayer correctly. Because there is a significant mismatch between the length of the HA TMD and the thickness of the ER membrane, it is conceivable that heavy truncations of the CT may cause a tilting or immersion of the hydrophobic TMD into the core of the membrane with severe consequences for the protein properties and function. An additional anchoring of the C-terminus on the cytoplasmic face of the membrane by palmitoylation or charged residues might prevent that process. In agreement with such hypothesis is the observation that addition of one highly hydrophilic residue (R558) is sufficient to at least partially restore the transport to the cell surface (Δ2S + R: Figs 2B, 3J and 4). We therefore conclude that the CT is a fundamental element for the delivery of the HA chimera to the PM. We are aware that our results are not in line with those published by Doyle (Doyle *et al*., 1986) reporting that 17 residues of the hydrophobic anchor are sufficient to assure the efficient transport of HA chimeras to the cell surface, thus excluding the involvement of the CT in such a process. However, different observations were made by Doyle in another study (Doyle *et al*., 1985). Here, changes in the CT of influenza virus HA were demonstrated to have a significant impact on the protein properties including intracellular trafficking and exit from the ER. It has to be pointed out that different virus influenza subtypes were used in the two studies by Doyle and the experiments presented here. Whereas the lab-adapted strain X-31 (H3N2) was used in the second study (Doyle *et al*., 1986), the initial report (Doyle *et al*., 1985) was based on A/Japan/305/57 (H2N2), and the present study employs constructs derived from A/FPV/Rostock/34 (H7N1). This fact may not only explain the allegedly conflicting results but might furthermore suggest different mechanism of protein stabilization exploited by different influenza subtypes.

It has to be pointed out, nevertheless, that the constructs used in the present work contain only a small fragment of the ectodomain, and it cannot be excluded that essential elements necessary for a correct protein folding and subsequent exit from the ER might be localized in this portion of HA. However, even if that objection is true, our data clearly demonstrate that this putative folding defect can be compensated by a complete and functional CT. A similar partly palmitoylation-dependent mechanism ensuring a systematic delivery of the δ opioid receptor to the plasma membrane has been recently observed (Petäjä-Repo *et al*., 2006).

Secondly, we could demonstrate by FLIM-FRET that one specific palmitoylation, namely, at C551 is sufficient for plasma membrane raft association of the protein (Fig. 5: compare Δ1 and Δ1S). Two independent series of constructs that provided coherent results were generated. For one series, only point mutations were inserted producing the protein wtC562S, wtC559S and wtC551S. For the other series, we truncated the protein sequence after the second (Δ1) or the first (Δ2) cysteine residue. Whereas deletion of the palmitoylation at C551 could be compensated by the remaining CT including the two other palmitoylations (Fig. 5: wtC551S), introduction of the C551S mutation in the truncated Δ1 variant completely abolished raft association (Fig. 5: Δ1S). Such results therefore indicate that the strongest contribution to raft association of HA chimeras is given by S-acylation at position 551, at least in the context of a truncated CT. The cysteine at this position is complexed with a stearate (Kordyukova *et al*., 2008), a longer fatty acid than palmitate. This may induce a deeper penetration into the bilayer and hence assuring a stronger association to lipid microdomains. We surmise that whereas stearate is

critically involved in lipid raft association of HA, the other two palmitic acid residues may be also required for interacting with the other viral proteins, in order to assure the efficient assembly of viral particles prior to budding (Enami and Enami, 1996; Ali *et al*., 2000; Chen *et al*., 2005). Notably, our results correlate with raft association data based on Triton X-100 insolubility obtained by (Chen *et al*., 2005). Although in recent years the method utilized herein is believed to be prone to artefacts and experimental observations are taken with caution, it is striking that their results, obtained with expressed HA, are in strong agreement with our finding that either C551 or both other palmitoylations are required for raft localization to occur. Interestingly, in the context of virus infection, Chen and others (Chen *et al*., 2005; Wagner *et al*., 2005) found the palmitoylation dependence of HA lateral sorting to be significantly different. This might indicate that other viral components interacting with the HA CT confer an independent raft-affinity factor to the protein and therefore compensate palmitoylation defects.

Thirdly, we performed FLIM-FRET experiments aiming at proteins in the Golgi apparatus and found clustering of our wt with the raft marker GPImCFP (Fig. 6). The mutant wtC3S on the other hand, although showing an intracellular distribution comparable with wt (Fig. 3K and Fig. 4), was again shown to produce much lower FRET, demonstrating that energy transfer in the Golgi apparatus is still reflective of raft association. Interestingly, the chimeras Δ1 and Δ2 possessed a reduced raft association in the Golgi apparatus compared with wt (Fig. 6), whereas at the plasma membrane, all three proteins partitioned to the same extent. We surmise that this finding is indicative of a lower occurrence, or a different composition of the lipid rafts in the Golgi apparatus because of the lower cholesterol content in this compartment with respect to the plasma membrane (Mallat, 1989). We suggest that, as a result of that, the raft partitioning of transmembrane proteins might be more sensitive in the Golgi apparatus to the abolishment of individual raft association factors such as palmitoylation.

Importantly, several recent publications reported a significant contribution of factors in the ectodomain to the raft partitioning of HA (Takeda *et al*., 2003; Engel *et al*., 2010; de Vries *et al*., 2015). However, although mutation of those elements clearly decreased the raft association and intracellular transport of HA (de Vries *et al*., 2015), they were found not to be sufficient to sustain lateral sorting upon an additional mutation of the cytoplasmic cysteins (Engel *et al*., 2010). We believe that this observation is indicative of a high degree of cooperativity between different raft targeting signals of HA. Most likely, the nanodomain association provided by HA palmitoylations is supported by, i.e. the putative cholesterol-binding elements in the ectodomain (de Vries *et al*., 2015) and vice versa. It is conceivable that those different elements add to the overall raft affinity of the protein and by that mediate a fine-tuning of the lateral sorting or provide a leaflet coupling for raft-dependent processes. We want to point out that our results might suggest a partial interconnection between raft association and intracellular distribution. In our study, several variants shown to be deficient in lipid raft partitioning were also found to possess a significant trafficking defect and were highly excluded from Golgi apparatus and plasma membrane (Δ1S, Δ2S: Figs 3G and I, 4 and 5). This might indicate a correlation between raft-affinity and plasma membrane localization as suggested by (Diaz-Rohrer *et al*., 2014). However, at least in our hands, a strict dependence of the plasma membrane localization on raft association can be excluded, because HA was found to be able to get access to the plasma membrane even if raft partitioning was completely abrogated (wtC3S: Figs 3K, 4 and 5).

Experimental procedures

Transmembrane domain-hemagglutinin constructs

Transmembrane domain-HA chimeric proteins were produced as described by (Scolari *et al*., 2009). Briefly, the HA sequence consisting of the TMD and CT as well as of 38 amino acid of the ectodomain of HA from A/FPV/Rostock/34 (H7N1), uniprot entry: P03459, corresponding to ASIRNNTYDHSKYREEAMQNRIQIDPVKLSGYKDV IL**WFSFGASCFLLLAIAMGLVFIC**VKNGNMRCTICI (glycosylation site, single underlined; palmitoylation site, double underlined; TMD, bold) was tagged on its N-terminus with mYFP (where m indicates mutation A206K inserted to prevent dimerization of fluorescent proteins) and expressed in CHO-K1 cells. Point mutations C551S, C559S and C562S were inserted into the sequence by overlap extension PCR (Urban *et al*., 1997; Kirsch *et al*., 1998), whereas Δ mutants and C3S-R558A were produced by conventional PCR.

Fluorescent marker and marker protein

The raft marker GPImCFP was produced as described by (Scolari *et al*., 2009), based on the sequence of GPI-CFP kindly provided by (Keller *et al*., 2001). The Golgi marker Golgi-turquoise generated by Dorus Gadella (as described in Goedhart *et al*., 2012) and GFP-Rab5 originally generated by Ron Vale and subcloned into an mTurquoise expression vector were assessed from Addgene (plasmids #31733 and #36205). All constructs were transfected in CHO-K1 cells using Lipofectamine 2000 (Invitrogen, Carlsbad, CA) according to the manufacturer protocol, and imaging was carried out about 24 h post-transfection. The endoplasmic reticulum was stained using ER-Tracker Red (Invitrogen).

Confocal and FLIM-FRET imaging

Intensity measurements as well as FLIM-FRET measurements were carried out as described by us previously (Scolari *et al*., 2009; Schwarzer *et al*., 2014). Briefly, an inverted FluoView 1000 microscope (Olympus, Tokyo, Japan) equipped with a time-resolved LSM upgrade Kit (PicoQuant, Berlin, Germany) and a 60× (1.35 N.A.) oil-immersion objective at 25°C was used. Images with a frame size of 512 × 512 pixels were acquired. FLIM was used to study energy transfer between the GPImCFP raft marker (donor) and the different TMD-HA-YFP variants (acceptor). CFP was excited at 440 nm using a laser diode and detected in the range 460–490 nm. YFP was excited at 515 nm using an argon laser and detected in the range 535–575 nm. The CFP lifetime of cells expressing only GPImCFP was first measured. Selection of cells co-expressing both proteins was based on the fluorescence emission in the CFP and YFP channels after sequential excitation. FLIM images of donor and donor in presence of acceptor were acquired upon excitation of the donor at 440 nm. Fluorescence intensities were analysed with ImageJ, enabling selection and analysis of the same area for pictures taken sequentially. For FLIM measurements, CFP was excited at 440 nm using a pulsed laser diode. The fluorescence was detected by a single photon avalanche photodiode and a 470 ± 15 nm bandpass filter. Electrical signals were processed by the TimeHarp 200 PC card (PicoQuant, Berlin, Germany). Analysis of the FLIM images was performed using the SymPhoTime software (PicoQuant, Berlin, Germany), taking into account the instrument response function. FLIM pictures were accumulated for 90 s (60 frames with an average photon count rate of $< 2–4 \times 10^4$ counts/s), and the plasma membrane was selectively analysed. The measured photons per pixels corresponding to the plasma membrane were combined into a decay curve that was further analysed by fitting it using a nonlinear least squares iterative procedure, as the sum of two exponential terms. This kind of fitting is required because fluorescent proteins variants are known to show a multiple exponential decay (Lakowicz, 2006). For every single cell, the average lifetime of CFP was calculated using the equation

$$\tau_{Av} = \frac{\sum_i \alpha_i \tau_i}{\sum_i \alpha_i},$$

where τ_{av} is the amplitude average weighted lifetime, α is the amplitude of a lifetime component and τ is the corresponding lifetime. Quality of fits was judged by the distribution of the residuals and the χ^2 value. The efficiency of FRET (E) was calculated using the equation

$$E(\%) = 1 - \frac{\tau_{DA}}{\tau_D}.$$

E (%) represents the relative FRET efficiency, τ_{DA} the average weighted lifetime of donor in presence and τ_D in absence of the acceptor. The FRET efficiency E (%) of every cell co-expressing donor and acceptor was plotted against the fluorescence intensity of the acceptor in this cell in order to generate the E (%) versus acceptor concentration plots.

Quantitative membrane expression analysis

To assess quantitative information about the relative plasma membrane expression of fusion protein, confocal images were analysed using ImageJ as described in (Schwarzer *et al*., 2014). Initially, cells were transfected with GPImCFP as a plasma membrane marker and the protein under study. Then, regions of interest were defined in the CFP images to select for the plasma membrane and the whole cell respectively. Assuming a direct proportion between acceptor concentration and fluorescence signal, normalized and background corrected YFP intensities were obtained, and the plasma membrane to overall ratio was calculated as a measure of the surface exposure. For every protein, 10 to 30 cells were analysed.

References

Ali, A., Avalos, R.T., Ponimaskin, E., and Nayak, D.P. (2000) Influenza virus assembly: effect of influenza virus glycoproteins on the membrane association of M1 protein. *J Virol* **74**: 8709–8719.

Armstrong, R.T., Kushnir, A.S., and White, J.M. (2000) The transmembrane domain of influenza hemagglutinin exhibits a stringent length requirement to support the hemifusion to fusion transition. *J Cell Biol* **151**: 425–437.

Backovic, M., and Jardetzky, T.S. (2011) Class III viral membrane fusion proteins. In *Adv Exp Med Biol* **714**: 91–101.

Brack, A.R., Klupp, B.G., Granzow, H., Tirabassi, R., Enquist, L.W., and Mettenleiter, T.C. (2000) Role of the cytoplasmic tail of pseudorabies virus glycoprotein E in virion formation. *J Virol* **74**: 4004–4016.

Brett, K., Kordyukova, L.V., Serebryakova, M.V., Mintaev, R.R., Alexeevski, A.V., and Veit, M. (2014) Sit#@e-specific S-acylation of influenza virus hemagglutinin The location of the acylation site relative to the membrane border is the decisive factor for attachment of stearate *. **289**: 34978–34989.

Campbell, S.M., Crowe, S.M., and Mak, J. (2002) Virion-associated cholesterol is critical for the maintenance of HIV-1 structure and infectivity. *AIDS* **16**: 2253–2261.

Chen, B.J., Takeda, M., and Lamb, R.A. (2005) Influenza virus hemagglutinin (H3 subtype) requires palmitoylation of its cytoplasmic tail for assembly: M1 proteins of two subtypes differ in their ability to support assembly. *J Virol* **79**: 13673–13684.

Copeland, C. (1986) Assembly of influenza haemagglutinin trimers and its role in intracellular transport. *J Cell Biol* **103**: 1179–1191.

Diaz-Rohrer, B.B., Levental, K.R., Simons, K., and Levental, I. (2014) Membrane raft association is a determinant of plasma membrane localization. *Proc Natl Acad Sci U S A* **111**: 8500–8505.

Doyle, C., Roth, M.G., Sambrook, J., and Gething, M.J. (1985) Mutations in the cytoplasmic domain of the influenza virus hemagglutinin affect different stages of intracellular transport. *J Cell Biol* **100**: 704–714.

Doyle, C., Sambrook, J., and Gething, M.J. (1986) Analysis of progressive deletions of the transmembrane and cytoplasmic domains of influenza hemagglutinin. *J Cell Biol* **103**: 1193–1204.

Enami, M., and Enami, K. (1996) Influenza virus hemagglutinin and neuraminidase glycoproteins stimulate the membrane association of the matrix protein. *J Virol* **70**: 6653–6657.

Engel, S., Scolari, S., Thaa, B., Krebs, N., Korte, T., Herrmann, A., and Veit, M. (2010) FLIM-FRET and FRAP reveal association of influenza virus haemagglutinin with membrane rafts. *Biochem J* **425**: 567–573.

Engel, S., Vries, M. De, Herrmann, A., and Veit, M. (2012) Mutation of a raft-targeting signal in the transmembrane region retards transport of influenza virus hemagglutinin through the Golgi. *FEBS Lett* **586**: 277–282.

Garten, W., Will, C., Buckard, K., Kuroda, K., Ortmann, D., Munk, K., *et al*. (1992) Structure and assembly of hemagglutinin mutants of fowl plague virus with impaired surface transport. *J Virol* **66**: 1495–1505.

Goedhart, J., von Stetten, D., Noirclerc-Savoye, M., Lelimousin, M., Joosen, L., Hink, M.A., *et al*. (2012) Structure-guided evolution of cyan fluorescent proteins towards a quantum yield of 93%. *Nat Commun* **3**: 751.

Gottlieb, T.A., Gonzalez, A., Rizzolo, L., Rindler, M.J., Adesnik, M., and Sabatini, D.D. (1986) Sorting and endocytosis of viral glycoproteins in transfected polarized epithelial cells. *J Cell Biol* **102**: 1242–1255.

Greaves, J., and Chamberlain, L.H. (2007) Palmitoylation-dependent protein sorting. *J Cell Biol* **176**: 249–254.

Harman, A., Browne, H., and Minson, T. (2002) The transmembrane domain and cytoplasmic tail of herpes simplex virus type 1 glycoprotein H play a role in membrane fusion. *Society* **76**: 10708–10716.

Hundt, M., Harada, Y., De Giorgio, L., Tanimura, N., Zhang, W., and Altman, A. (2009) Palmitoylation-dependent plasma membrane transport but lipid raft-independent signaling by linker for activation of T cells. *J Immunol* **183**: 1685–1694.

Januszeski, M.M., Cannon, P.M., Chen, D., Rozenberg, Y., and Anderson, W.F. (1997) Functional analysis of the cytoplasmic tail of Moloney murine leukemia virus envelope protein. *J Virol* **71**: 3613–3619.

Jin, H., Leser, G.P., Zhang, J., and Lamb, R.A. (1997) Influenza virus hemagglutinin and neuraminidase cytoplasmic tails control particle shape. *EMBO J* **16**: 1236–1247.

Keller, P., Toomre, D., Díaz, E., White, J., and Simons, K. (2001) Multicolour imaging of post-Golgi sorting and trafficking in live cells. *Nat Cell Biol* **3**: 140–149.

Kielian, M., and Rey, F.A. (2006) Virus membrane-fusion proteins: more than one way to make a hairpin. *Nat Rev Microbiol* **4**: 67–76.

Kirsch, R.D., Joly, E. (1998) An improved PCR-mutagenesis strategy for two-site mutagenesis or sequence swapping between related genes. *Nucleic Acids Research* **26**(7): 1848–1850.

Kordyukova, L.V., Serebryakova, M.V., Baratova, L.A., and Veit, M. (2008) S acylation of the hemagglutinin of influenza viruses: mass spectrometry reveals site-specific attachment of stearic acid to a transmembrane cysteine. *J Virol* **82**: 9288–9292.

Lakowicz, J.R. (2006) Principles of fluorescence spectroscopy.

Mallat, S.G. (1989) Theory for multiresolution signal decomposition: the wavelet representation. *IEEE Trans Pattern Anal Mach Intell* **11**: 674–693.

Murakami, T., and Freed, E.O. (2000) The long cytoplasmic tail of gp41 is required in a cell type-dependent manner for HIV-1 envelope glycoprotein incorporation into virions. *Proc Natl Acad Sci U S A* **97**: 343–348.

Oomens, A.G.P., Bevis, K.P., and Wertz, G.W. (2006) The cytoplasmic tail of the human respiratory syncytial virus F protein plays critical roles in cellular localization of the F protein and infectious progeny production. *J Virol* **80**: 10465–10477.

Petäjä-Repo, U.E., Hogue, M., Leskelä, T.T., Markkanen, P.M.H., Tuusa, J.T., and Bouvier, M. (2006) Distinct subcellular localization for constitutive and agonist-modulated palmitoylation of the human δ opioid receptor. *J Biol Chem* **281**: 15780–15789.

Resh, M.D. (2004) Membrane targeting of lipid modified signal transduction proteins. In *Subcell Biochem* **37**: 217–232.

Rindler, M.J., Ivanov, I.E., Plesken, H., Rodriguez-Boulan, E., and Sabatini, D.D. (1984) Viral glycoproteins destined for apical or basolateral plasma membrane domains transverse the same Golgi apparatus during their intracellular transport in Madin–Darby canine kidney cells. *J Cell Biol* **98**: 1304–1319.

Roberts, P.C., Garten, W., and Klenk, H.D. (1993) Role of conserved glycosylation sites in maturation and transport of influenza A virus hemagglutinin. *J Virol* **67**: 3048–3060.

Rodriguez-Boulan, E., Paskiet, K.T., Salas, P.J., and Bard, E. (1984) Intracellular transport of influenza virus hemagglutinin to the apical surface of Madin–Darby canine kidney cells. *J Cell Biol* **98**: 308–319.

Scheiffele, P., Roth, M.G., and Simons, K. (1997) Interaction of influenza virus haemagglutinin with sphingolipid-cholesterol membrane domains via its transmembrane domain. *EMBO J* **16**: 5501–5508.

Schwarzer, R., Levental, I., Gramatica, A., Scolari, S., Buschmann, V., Veit, M., and Herrmann, A. (2014) The cholesterol-binding motif of the HIV-1 glycoprotein gp41 regulates lateral sorting and oligomerization. *Cell Microbiol* **16**: 1565–1581.

Scolari, S., Engel, S., Krebs, N., Piazzo, A.P., De Almeida, R. F.M., Prieto, M., *et al*. (2009) Lateral distribution of the transmembrane domain of influenza virus hemagglutinin revealed by time-resolved fluorescence imaging. *J Biol Chem* **284**: 15708–15716.

Simons, K., and Sampaio, J.L. (2011) Membrane organization and lipid rafts. *Cold Spring Harb Perspect Biol* **3**: 1–17.

Smotrys, J.E., and Linder, M.E. (2004) Palmitoylation of intracellular signaling proteins: regulation and function. *Annu Rev Biochem* **73**: 559–587.

Steven, A.C., and Spear, P.G. (2006) Biochemistry. Viral glycoproteins and an evolutionary conundrum. *Science* **313**: 177–178.

Surma, M.A., Klose, C., and Simons, K. (2012) Lipid-dependent protein sorting at the trans-Golgi network. *Biochim Biophys Acta – Mol Cell Biol Lipids* **1821**: 1059–1067 Doi: 10.1016/j.bbalip.2011.12.008

Takeda, M., Leser, G.P., Russell, C.J., and Lamb, R.A. (2003) Influenza virus hemagglutinin concentrates in lipid raft microdomains for efficient viral fusion. *Proc Natl Acad Sci U S A* **100**: 14610–14617.

Urban, A., Neukirchen, S., and Jaeger, K. (1997) A rapid and efficient method for site-directed mutagenesis using one-step overlap extension PCR. *Nucl Acids Res* **25**(11): 2227–2228.

Veit, M. (2012) Palmitoylation of virus proteins. *Biol Cell* **104**: 493–515.

Veit, M., Kretzschmar, E., Kuroda, K., Garten, W., Schmidt, M.F., Klenk, H.D., and Rott, R. (1991) Site-specific mutagenesis identifies three cysteine residues in the cytoplasmic tail as acylation sites of influenza virus hemagglutinin. *J Virol* **65**: 2491–2500.

Veit, M., Söllner, T.H., and Rothman, J.E. (1996) Multiple palmitoylation of synaptotagmin and the t-SNARE SNAP-25. *FEBS Lett* **385**: 119–123.

Vetrivel, K.S., Cheng, H., Lin, W., Sakurai, T., Li, T., Nukina, N., *et al*. (2004) Association of gamma-secretase with lipid rafts in post-Golgi and endosome membranes. *J Biol Chem* **279**: 44945–44954.

de Vries, M., Herrmann, A., and Veit, M. (2015) A cholesterol consensus motif is required for efficient intracellular transport and raft association of a group 2 HA from influenza virus. *Biochem J* **465**: 305–314.

Wagner, R., Herwig, A., Azzouz, N., and Klenk, H.D. (2005) Acylation-mediated membrane anchoring of avian influenza virus hemagglutinin is essential for fusion pore formation and virus infectivity. *J Virol* **79**: 6449–6458.

Wagner, R., Heuer, D., Wolff, T., Herwig, A., and Klenk, H.D. (2002) N-Glycans attached to the stem domain of haemagglutinin efficiently regulate influenza A virus replication. *J Gen Virol* **83**: 601–609.

Wilson, I.A., Skehel, J.J., and Wiley, D.C. (1981) Structure of the haemagglutinin membrane glycoprotein of influenza virus at 3 A resolution. *Nature* **289**: 366–373.

Zacharias, D.A., Violin, J.D., Newton, A.C., and Tsien, R.Y. (2002) Partitioning of lipid-modified monomeric GFPs into membrane microdomains of live cells. *Science* **296**: 913–916.

Zhang, J., Pekosz, A., and Lamb, R.A. (2000) Influenza virus assembly and lipid raft microdomains: a role for the cytoplasmic tails of the spike glycoproteins. *J Virol* **74**: 4634–4644.

Supporting information

Additional Supporting Information may be found in the online version of this article at the publisher's web-site:

Fig. S1. Intracellular distribution of HAmYFP and unlabeled HA. Representative confocal images of cells transfected with (A) HAmYFP or (B) unlabeled HA upon immunofluorescence staining using anti-HA antibodies. The yellow lines in the second and third columns display the regions of interest used for relative surface expression analysis, namely plasma membrane and entire cell, respectively. The numbers in the last column indicate the relative surface exposure, as quotient of plasma membrane fluorescence and overall fluorescence of the individual cell images.

Fig. S2. Intracellular localization of unlabeled, full-length HA in CHO-K1 cells. Confocal images of cells transfected with HA and Golgi-Turquoise or HA alone respectively, upon immunofluorescence staining against HA or against HA and endogenous membrin as alternative marker of the Golgi apparatus. Insets show a magnified region of the boxed area.

Fig. S3. Microscopic characterization of Δ2. Confocal images of CHO-K1 cells transfected with Δ2 (A) upon staining with ER-Tracker Red and upon co-transfection with the proteins (B) Golgi-Turquoise or (C) Rab5-Turquoise. The latter served as a marker of endocytic vesicles. Insets show a magnified region of the boxed area.

Fig. S4. Analysis of raft clustering of HA variants. The FRET efficiencies of individual cells were plotted against their respective acceptor intensities to validate nanodomain clustering. At least 20 cells of each construct were analyzed. FRET saturation fits (black lines) were generated according to the model previously published Zacharias et al., 2002. Fitting Parameters are stated in the bottom tables of each plot.

Fig. S5. Palmitoylation of HA variants. Protein chimeras were labelled with 3H-palmitic acid or 35S-methionine (35S-Met) for 4 h, immunoprecipitated with anti-GFP antibodies and subjected to non-reducing SDS–PAGE and fluorography. (A) Wildtype and single palmitolylation mutants. (B) Wildtype and palmitoylation triple mutant.

Fig. S6. Quantification of construct expression at the plasma membrane. Intensity ratio of donor to acceptor (D/A) for different constructs co-transfected with GPImCFP. Data represent the mean ± S.E.